KINETICS, CATALYSIS, AND REACTION ENGINEERING

Pyrolysis Reaction Mechanism for Industrial Naphtha Cracking Furnaces

Eunjung Joo and Sunwon Park*

Department of Chemical Engineering, Korea Advanced Institute of Science and Technology, 373-1 Kusong-dong, Yusong-ku, Taejon 305-701, Korea

Moonyong Lee

School of Chemical Engineering and Technology, Yeungnam University, Kyongsan 712-749, Korea

The tough market situation for ethylene production has accelerated the development of a more rigorous and reliable cracking model. However, thermal cracking of naphtha has such numerous reaction routes and intermediate radicals and molecules that the detailed reaction mechanism has not yet been determined. This research is aimed at developing a rigorous but practical reaction mechanism for an industrial cracker model. First, the reaction mechanism set for naphtha cracking is generated on the basis of major reaction classes in pyrolysis and feed components. To reduce the computational load, the reaction mechanism set is reduced using the eigenvalue−eigenvector decomposition method. To compensate for the uncertainty in the kinetic parameters for a plant, the mechanism is customized based on the results of a sensitivity analysis. The constructed reaction mechanism can be used to optimize the operating conditions of the naphtha cracker by precise estimation of the production yield of a given naphtha sample with a manageable computational load and flexibility toward industrial practices.

1. Introduction

Expansion in the petrochemical industry; continuing demands for ethylene, propylene, and butadiene; varying feedstock availability, and rapidly changing market situations have brought interest in and research into the modeling of naphtha pyrolysis reactors. The optimal design, optimal operating strategy, and purchase decisions for raw materials are becoming main issues in the ethylene industry. This kind of problem can be well-treated by a mechanistic kinetic model.[1]

For the development of well-balanced mechanistic models, it is necessary to know the reactions taking place in the reactor. Naphtha contains a large number of hydrocarbons, and because of the complexity of the feed and the radical nature of the reactions, thousands of reactions can occur among the various free-radical species. The preexponential factors and activation energies for most of these free-radical reactions are not precisely known. Although many investigators have measured the product yield in naphtha pyrolysis, very few detailed kinetic models have been published. Modeling of naphtha pyrolysis has been attempted at various levels of sophistication. The simplest model correlated the product yield with some parameters such as the cracking severity index[2]. On the other extreme are simulation programs based on the fundamental free-radical reaction kinetics.[3] Van Damme and Froment[4] created global disappearance models both for typical naphtha and for lumped components such as *n*-paraffin, isoparaffin, naphthene, and aromatics. They also devised a more detailed model based on the individual molecular reactions and initial selectivities for *n*-paraffins and isoparaffins obtained using the Rice and Kossiakoff theory.[5] The initial selectivities for naphthenes were estimated from the limited literature sources and their own experimental data. However, neither the details of the reaction scheme nor the numerical values of the various parameters such as the preexponential factors, the activation energies, and the initial selectivities were disclosed. Kumar and Kunzru[2] developed a pyrolysis model that contains 22 molecular reactions including aromatics. They revealed the reaction model so it can be used for various purposes, but their model has the limitation that the initial selectivities have to be determined experimentally. Van Damme and Froment[4] developed gross molecular reaction kinetics for three typical types (light, middle, and heavy) of naphtha experimentally. However, for proprietary reasons, no details have been disclosed.

Another issue in the modeling of naphtha pyrolysis is mapping of the feed from the commercial indices to the conventional components. Naphtha is a complicated hydrocarbon mixture, and thus, its characteristics are usually defined by normal inspection tests such as ASTM D86 boiling curves, specific gravities, and/or total *n*-paraffin/isoparaffin/naphthene/aromatics (PINA) weight fractions. Only the commercial software SPYRO has a characterization routine that converts these commercial indices into detailed components used in the kinetic scheme through iterative empirical correlations.[6]

* To whom all correspondence should be addressed. E-mail: swpark@mail.kaist.ac.kr. Fax:+82-42-869-3910.

10.1021/ie000774o CCC: $20.00
Published on Web 05/01/2001

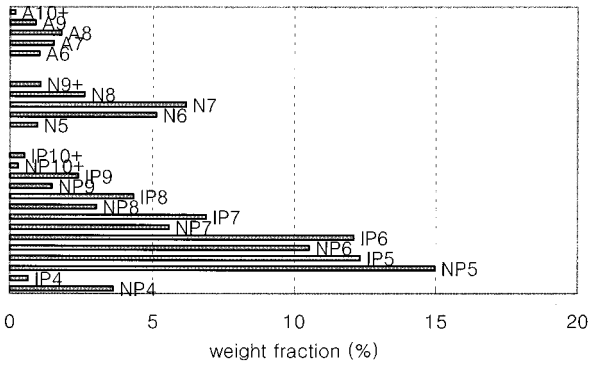

Figure 1. Industrial naphtha analysis.

The aim of this study is to develop a naphtha pyrolysis reaction model that can be used to predict the yields of major products from a given naphtha sample with commercial indices. With the aid of the kinetic theories and previous research, a major reaction network is generated according to the major feed components and reaction classes. The generated reaction mechanism is reduced by extracting meaningful kinetic information using the eigenvalue−eigenvector decomposition method so that the overall computational load of a full cracker model can be maintained within a practical level. Several important kinetic parameters are chosen from the sensitivity analysis and optimized to customize the model to specific plant data.

2. Mechanism Generation

2.1. Selection of Major Components. To determine the species to be considered in the reaction model, the feed material, industrial naphtha, was analyzed and averaged for 140 cases. The analysis was performed on normal paraffin 4 (NP4), NP5, NP6, NP7, NP8, NP9, NP10+, isoparaffin 4 (IP4), IP5, IP6, IP7, IP8, IP9, IP10+, naphthene 5 (N5), N6, N7, N8, N9+, aromatics 6 (A6), A7, A8, A9, and A10+. The average weight fractions are shown in Figure 1. According to the Figure 1, the considered naphtha can be regarded as light naphtha because the amount of large molecules higher than C_9 is relatively small. A wide range naphtha is known to have more $>C_9$ molecules, which have numerous reaction routes and generate many radicals. If more analysis data are available for the wider range of naphtha, the reaction mechanism can be extended to $>C_9$ to cover the wide range of naphtha. In this study, the feed components are restricted to NP/IP 4−8, and N 5−7, which covers 86.24% of the analyzed species. Furthermore, to select a representative configuration for each component that has isomers, more detailed analyses were performed on 60 components. As a result, 2-methyl-pentane for IP6, 2-methyl-hexane for IP7, 2-methyl-heptane for IP8, cyclopentane for N5, methylcyclopentane for N6, and methylcyclohexane for N7 were chosen as the representatives.

2.2. Generation of the Reaction Mechanism. To establish the reaction network, it is necessary to take into consideration the most important species and reactions. The main reaction classes of naphtha pyrolysis are shown in Table 1. By classifying the elementary reactions for a mechanistic model, the analogies for reactions of the same class can be applied. Thus, the number of kinetic parameters to be obtained can be reduced. Ranzi et al.[7,8] and Dente and Ranzi[1] showed that chain-initiation, hydrogen-abstraction, radical-decomposition, and radical-isomerization reactions are the primary reactions for naphtha pyrolysis.

Table 1. Main Reaction Classes of Naphtha Pyrolysis

1. Chain-initiation reactions
   $R-R' \rightarrow R^*+R'^*$
2. Hydrogen-abstraction reactions
   $R^*+R'H \rightarrow RH+R'^*$
3. Radical-decomposition reactions
   $R^* \rightarrow RH+R'^*$
4. Radical-addition reactions to unsaturated molecules
   $RH + R'^* \rightarrow R''^*$
5. Chain-termination reactions
   $R^* + R'^* \rightarrow R-R'$
6. Molecular reactions
   $RH + R'H \rightarrow R''H + R'''H$
7. Radical-isomerization reactions
   $R'^* \rightarrow R''^*$

Rice and Herzfeld developed a free-radical chain mechanism to explain the general features of paraffinic hydrocarbon decompositions.[9] However, the ethylene yield predicted by this R−H mechanism was much higher than the experimental results. To account for this discrepancy, Kossiakoff and Rice (R−K mechanism)[5] assumed that, prior to decomposition, the free radicals with long carbon skeletons isomerize instantaneously through internal hydrogen abstractions, with the formation of five-membered (1−4 transfer) or six-membered (1−5 transfer) rings. The results from the R−K mechanism exhibited relatively good agreement with experimental work. Murata and Saito[9] demonstrated the R−K mechanism using experimental results ranging from *n*-C_4 to *n*-C_{16}.

According to these theories, the reaction mechanism can be generated. However, the total numbers of elementary reactions and radicals can be too large. To reduce the total numbers of reactions and radicals to be considered, Ranzi et al.[7] introduced the important simplification that all intermediate radicals higher than C_4 are assumed to be transformed directly into their final products. The model showed fair or good agreement with the experimental results for the initial product distribution.[7] However, as the reaction proceeded, the simplification produced overpredictions of higher olefins and underpredictions of ethylene, propylene, and methane. To overcome this effect, it is necessary to add olefin-cracking reactions into the reaction mechanism set.

In short, the generated reaction mechanism is based on the following premises: (1) Free radicals are produced by the splitting of hydrocarbons at their weakest bonds. (2) Free radicals abstract hydrogen atoms from the hydrocarbon to form saturated molecules and new free radicals. (3) Radicals with a long carbon skeletons isomerize through internal hydrogen abstractions through the ring formation. (4) Radicals higher than or equal to C_4 stabilize themselves by splitting into their final products. (5) Only the radicals lower than C_4 are active radicals in the reactions. (6) Chain ending occurs through association and/or disproportionation of radicals.

As feed components are heavier hydrocarbon molecules ($>C_4$), their reactions are generated on the basis of the above premises starting from the initiation reactions of the feed components that were previously selected.

For the reactions of light hydrocarbons such as ethane, propane, and butane, many investigators have published the reaction mechanisms, so their reaction routes are relatively well-known. Dente and Ranzi[1]

Table 2. Kinetic Parameters for Paraffins[a]

H-Abstraction Reactions

H atom position	primary	secondary	tertiary
primary radical	$10^8 \exp(-13.5/RT)$	$10^8 \exp(-11.2/RT)$	$10^8 \exp(-9/RT)$
secondary radical	$10^8 \exp(-14.5/RT)$	$10^8 \exp(-12.2/RT)$	$10^8 \exp(-10/RT)$
tertiary radical	$10^8 \exp(-15/RT)$	$10^8 \exp(-12.7/RT)$	$10^8 \exp(-10.5/RT)$

Isomerization reactions

	five-membered ring	six-membered ring	seven-membered ring
primary radical	$10^{11} \exp(-20.6/RT)$	$10^{10.2} \exp(-14.5/RT)$	$10^{9.7} \exp(-14.5/RT)$

Decomposition Reactions to Form Primary Radicals

from primary radical	from secondary radical	from tertiary radical
$10^{14} \exp(-30/RT)$	$10^{14} \exp(-31/RT)$	$10^{14} \exp(-31.5/RT)$

Corrections in Activation Energy to Form Various Radicals

methyl radical	secondary radical	tertiary radical
+2	−2	−3

[a] From Ranzi et al.[7]

published 422 free-radical reactions involving 48 species for the cracking of an ethane and propane mixed feed. Tomlin et al.[10] reduced their reaction mechanism for propane cracking into 122 equivalent reactions using identification of redundant species and principal-component analysis of the local rate sensitivity matrix. They further reduced the mechanism to 50 reactions by removing fast reversible reactions. In this study, the reaction mechanisms for light hydrocarbons are based largely on these 50 reactions and also include more reactions for olefin cracking from Dente and Ranzi.[1]

Little information is available for the cracking reactions of naphthenes. Thus, the major reaction classes are applied to the naphthenes in a similar way. However, naphthenes do not have the long carbon skeletons, so the isomerization reactions are not considered.

2.3. Kinetic Parameter Assignment. For the generated reaction sets, the reaction kinetic parameters should be assigned. They can be obtained by experiment or from the open literature. However, for the complex naphtha-cracking reactions, there exist many reactions for which the kinetic parameters cannot be found in the open literature. In that case, the parameters can be obtained by exploiting structural or mechanistic analogies among similar reactions with a fairly limited number of truly independent kinetic parameters.[7] For example, with the most widely adopted analogy, it is assumed for H-abstraction reactions that the preexponential factor and activation energy depend only on the abstracting radical and the type of abstracted H atom, respectively. The reactions associated with paraffins are generated in full on the basis of Table 2. They have already been discussed for hydrocarbon pyrolysis.[1,7,8,11] The 4th part of the Table 2 provides corrections to the decomposition reactions that form not primary radicals but rather various radicals such as methyl, secondary, and tertiary radicals. For naphthenes, because of the lack of available kinetic data, the values of the parameters by Nigam and Klein[12] shown in Table 3 are used. They suggested a thermochemical kinetic-based lumping strategy to reduce the number of parameters to be determined by the experiments. This approach is useful when many kinetic parameters must be obtained with few experimental data because it determines the representative values of the kinetic parameter for the reaction classes. The differences among reactions in a reaction class are reflected by the heats of reaction. The details of the reaction kinetics can be found in Ranzi et al.[7] and Nigam and Klein.[12] The amounts of aromatics are relatively small, and their reactivities are low enough that they can be neglected or treated as inert species.[2,4] The initiation reactions are compiled from Allara and Shaw.[13] The data for the olefin-cracking, H-abstraction, radical-decomposition, radical-addition, chain-termination, and radical-isomerization reactions for molecules under C_4 are compiled from Dente and Ranzi[1] and Allara and Shaw.[13]

Table 3. Quantitative Structure−Reactivity Relationships for the Pyrolysis of Naphthenes[a,b]

reaction class	log(*A*)	E_a	
initiation	16.0	Δd^o	
H abstraction	8.5	$E_a = E_\alpha - \alpha q$ (exothermic reaction) $E_a = E_\alpha - (1-\alpha) q$ (endothermic reaction)	$E_\alpha = 16.2$, $\alpha = 0.13$
decomposition	13.0	$E_a = E_\beta - \beta q$	$E_\beta = 11.7$, $\beta = 0.28$

[a] From Nigam and Klein[12]. [b] Units = L mol s kcal.

The developed reaction mechanism with kinetic parameters includes 84 species (49 radicals and 35 molecules) and 365 reactions.

3. Mechanism Reduction

Models describing furnaces for the thermal cracking of naphtha need to combine the large number of reactions with complex heat- and material-transfer phenomena in the reactor, firebox, and preheating convection sections, which already entail a rather large computational load. Therefore, it is of practical importance that the model be constructed with the minimum computational load. The developed reaction mechanism set has several hundred reactions, some of which might be unimportant or redundant. The dimensions of the kinetic reactions can be reduced by a sensitivity analysis,[14] and the low-order reaction models can then be incorporated into the full physical model of the cracking furnace. The computational load can be reduced without loss of accuracy in the reaction model with a smaller number of reactions.

3.1. Sensitivity Analysis and Eigenvalue−Eigenvector Decomposition. A sensitivity analysis shows the effects on a model as a function of the parameters.

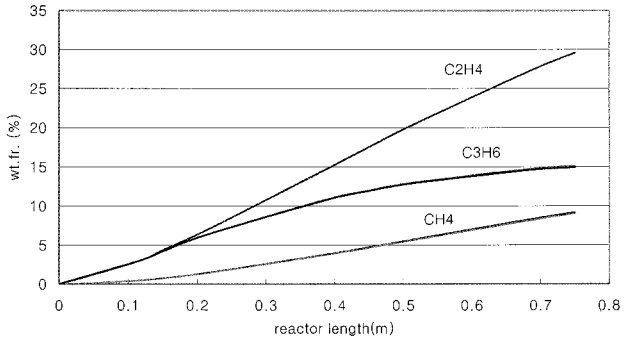

Figure 2. Comparison of weight fractions between full and reduced reaction models.

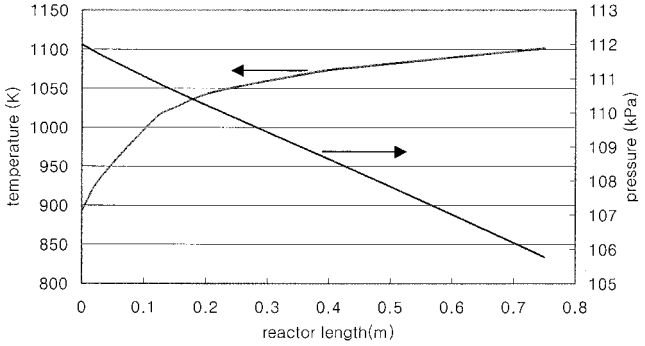

Figure 3. Comparison of temperature and pressure between full and reduced reaction models.

The normalized concentration sensitivity can be defined as

$$s_{ij} = \frac{k_j}{c_i}\frac{\partial c_i}{\partial k_j} = \frac{\partial \ln c_i}{\partial \ln k_j} \tag{1}$$

Sensitivities can be calculated at several points (times or axial positions) using Jacobian information obtained during the integration of the system differential equations.[15] In a chemical reaction system, kinetic parameters are usually changed simultaneously. The effect on the calculated behavior of a reaction mechanism can be expressed in terms of a function defined by

$$Q(\alpha) = \sum_{j=1}^{q}\sum_{i=1}^{m}\left[\frac{y_{ij}(\alpha) - y_{ij}(\alpha^0)}{y_{ij}(\alpha^0)}\right]^2 \tag{2}$$

where $\alpha = \ln k$; $y_{ij}(\alpha) = y_i(t_j,\alpha)$; and m and q denote the number of species and the number of points at which the sensitivity analysis is performed, respectively. A Taylor series expansion around the reference point α^0 and an eigenvalue−eigenvector decomposition can transform this function into the equation

$$\tilde{Q}(\Psi) = \sum_{i=1}^{p}\lambda_i(\Delta\Psi_i)^2 \tag{3}$$

where λ_i is the eigenvalue and $\Delta\Psi = U^T(\Delta\alpha)$. U is the normalized eigenvector matrix such that $u_i^T u_i = 1$, $\Delta\alpha = \alpha - \alpha^0$, and the principal component $\Psi = U^T\alpha$. Let u_1 denote the eigenvector of the largest eigenvalue λ_1; then, $\Delta\Psi_1 = (u_{1,1}\Delta\alpha_1 + \cdots + u_{1,p}\Delta\alpha_p)$. Selecting $\Delta\alpha_i = \ln(k_i/k_i^0) = u_{1,i}$ gives $\Delta\Psi_1 = 1$ and $\Delta\Psi_i = 0$ for $i \neq 1$ because of the orthogonality of eigenvectors. Therefore, eq 3 becomes $\tilde{Q}(\Psi) = \lambda_1$. If $u_{1,j} \leq 0.1$, then $\Delta\alpha_j$ contributes less than 1% to this effect.

If we set $|\Delta y_{i,j}|/y_{i,j} \leq 0.01$ for each i and j, then, from eq 2, we find

$$\tilde{Q}(\alpha) = \lambda_i \leq mq \times 10^{-4} \tag{4}$$

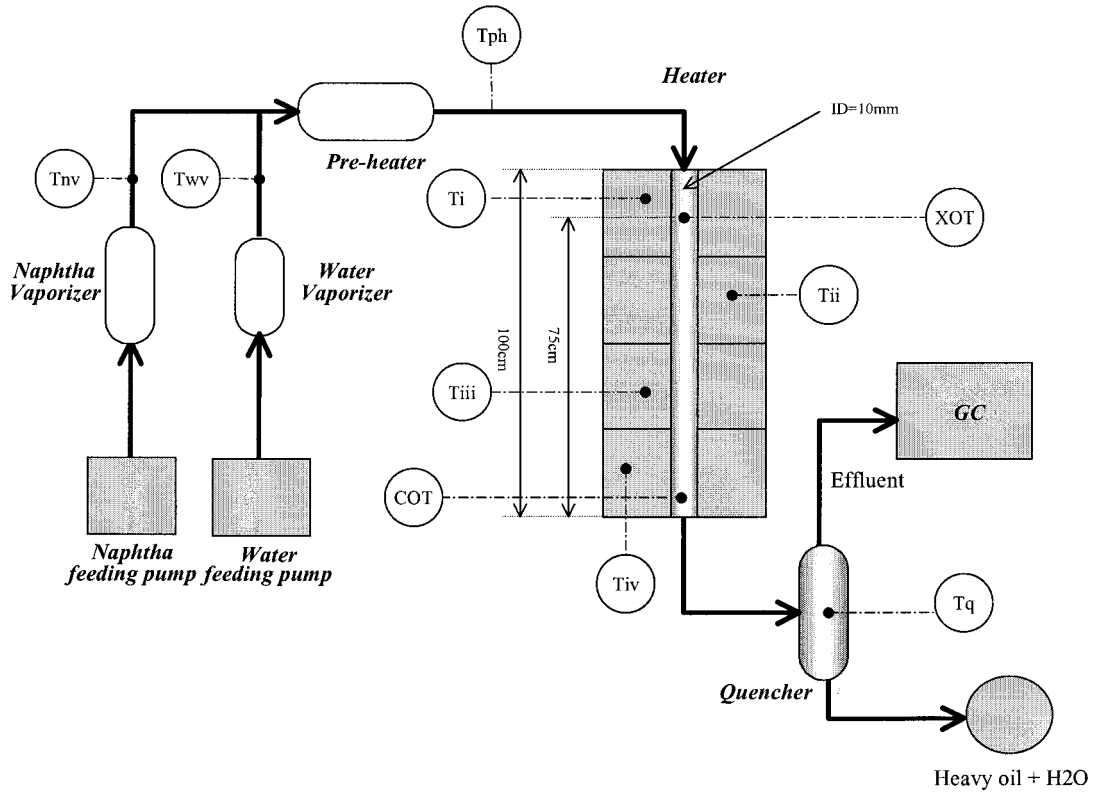

Figure 4. Simplified diagram of pilot plant under the consideration.

This result means that the largest eigenvalue that satisfies this equation would affect the error function by less than 1%. More specifically, the reactions that are the components of the eigenvectors for that eigenvalue would affect the error function by less than 1%. Therefore, reactions that appear for the first time in those ranges of eigenvalue and eigenvector can be eliminated without significant error. The details can be found in Turanyi.[16]

3.2. Reduced Mechanism. By selecting $|\Delta y_{i,j}|/y_{i,j} \leq 0.005$ and $u_{1,j} \leq 0.1$, the full reaction mechanism can be successfully reduced from 365 reactions to 231 reactions and from 84 species to 79 species. The results are shown in Figures 2 and 3. Simulation results for full reaction model that has 365 reactions are coincident with those for reduced reaction model that has 231 reactions: the results of the reduced model cannot be distinguished from those of the full model in Figures 2 and 3.

4. Mechanism Customization

The generated reactions show the qualitative trend of the reactor successfully. However, the simulation results might be different from the real plant data because of the specific characteristics of the plant under consideration. In that case, it is helpful to fit the reaction model to the plant by adjusting several dominant kinetic parameters. In this study, experimental data for a pilot plant were collected, and the resulting customization of the reaction model is presented below.

4.1. Description of Pilot Plant. The operating data were collected from the pilot plant shown in Figure 4. The crossover temperature and the tube metal temperature can be controlled in the pilot plant. During operation, the tube metal temperature at each section of the reactor was maintained at a constant temperature and monitored by the indicators T_i, T_{ii}, T_{iii}, and T_{iv}. The process temperatures at both the inlet and the outlet of the reactor were also measured by the indicators XOT and COT, respectively. Operating data were collected for various operating conditions of feed flow rate, steam/oil ratio, tube metal temperature, and crossover temperature.

4.2. Selection of Important Reactions. Customization of the reaction model means adjusting several kinetic parameters to estimate the temperature and composition of the most important components with precision. Therefore, the first issue is to identify the most dominant kinetic parameters associated with the major variables selected. In this study, through the sensitivity analysis for the products ethylene and propylene by SENKIN[15] and KINALC,[16] the most important reactions were identified as

$$C_2H_5 \rightarrow C_2H_4 + H \quad (1)$$

$$C_3H_7 \rightarrow C_2H_4 + CH_3 \quad (2)$$

$$C_3H_7 \rightarrow C_3H_6 + H \quad (3)$$

All of the reactions have kinetic parameters in Arrhenius form. Because the kinetic reaction rate is more sensitive to the activation energy than the preexponential factor, the activation energies of these three reactions were selected as the optimizing variables in this parameter optimization problem.

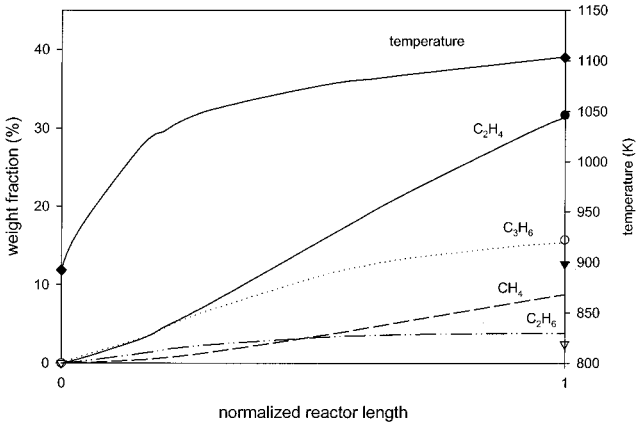

Figure 5. Comparisons between simulation results and operating data. Lines denote simulation data, and symbols denote operating data.

4.3. Optimization of Kinetic Parameters. The objective function shown in eq 10 represents the difference between the simulation results and operating data at the end of the reactor. The decision variables are the activation energies of the three previously determined reactions. The constraints are the general governing equations of the reactor in eq 11.

$$\min_{E_a} \sum_{i=1}^{\text{set \#}} \{[y_f(T) - y_T^o]_i^2 + [y_f(C_2H_4) - y_{C_2H_4}^o]_i^2 + [y_f(C_3H_6) - y_{C_3H_6}^o]_i^2\} \quad (10)$$

subject to

$$-W\frac{\partial g_i}{\partial z} + \sum_{j=1}^{m} f_{ij}\mathrm{MW}_i = \rho\frac{\partial g_i}{\partial t}$$

$$\rho C_p\left(\frac{\partial T}{\partial t} + V\frac{\partial T}{\partial z}\right) = \frac{\partial p}{\partial t} + \sum_{j=1}^{m}(-\Delta H_j)f_j + \frac{\alpha UP}{A}(T_a - T)$$

$$-W\frac{\partial V}{\partial z} - \frac{\partial p}{\partial z} - \frac{P}{A}\rho V^2 f = \rho\frac{\partial V}{\partial t}$$

$$\sum_{i=1}^{NC} g_i = 1.0$$

$$V = W/\rho$$

$$f_j = \sum_i \nu_{ij} f_{ij}$$

$$f_{ij} = k_j \prod_l C_l^{|\nu_{lj}|} \quad \text{if} \quad \nu_{lj} < 0$$

$$k_j = A_j \exp(-E_{aj}/RT) \quad (11)$$

The optimization was performed by NPSOL,[17] and the DAEs were solved by DASSL[18] with the aid of Chemkin.[19] The necessary properties were based on the Chemkin database, and the missing properties were collected from several references.[20,21] The optimized values are shown in Table 4, and typical simulation results are shown in Figure 5. The customized kinetic reaction model is useful and valid only for this particular pilot plant. The simulation results are fairly successful for the ethylene, propylene, and temperature

Table 4. Optimized Values of the Activation Energies

activation energy (J/mol)	reaction 1	reaction 2	reaction 3
initial value	191207.9	142262.5	163183.9
optimized value	187065.0	141431.1	156527.7

profiles. The constructed reaction mechanism set can be found in http://pslab.kaist.ac.kr/~cracker/.

5. Feed Characterization

The constructed reaction mechanism is composed of conventional components. In the industrial field, however, naphtha is usually characterized by commercial indices such as ASTM boiling curves, paraffin/isoparaffin/naphthene/aromatics weight fractions (PINAs), and specific gravities. Therefore, a mapping from the commercial indices to the fractions of conventional components is necessary for use of the reaction mechanism. However, no details about a mechanistic mapping have been available so far. Because the kinetic mapping is known to be impossible, a data-driven empirical correlation approach could be more adequate. In this study, a neural network technique was chosen for construction of the feed characterization module because the relationship between the commercial indices and the conventional components is nonlinear. A standard multilayer feedforward neural network was trained with 230 feed data sets. The neural network consisted of three layers with 10 input nodes, 14 output nodes, and 14 hidden nodes. The input variables for the neural network were PINAs (weight fractions), ASTM boiling points (IBP, 10%, 50%, 90%, EBP), and specific gravities; the output variables were the weight fractions of the feed naphtha components that were selected as previously mentioned, namely, NP 4−8, IP 5−8, and N 5−7, and pseudo components that are assumed to be inactive in the reaction mechanism. The prediction performance of the neural network is extensively tested through cross-validation steps. As a result, the developed neural network model shows fairly good performance in predicting the conventional components from the commercial indices.

One of the main problems with a neural network approach is that the prediction reliability of the neural network is limited to the interpolation range of the tested input data set. In this study, to test the reliability of the results for new input, a principal-component analysis (PCA) was used in parallel with the neural network model. In multivariate statistics, it is necessary to understand a data set by considering a group of variables together, rather than by focusing on only one variable at a time. By replacing a group of variables with a single new variable, multidimensional problems can be classified. PCA is a quantitatively rigorous method for this purpose. The newly defined variables, or principal components, reduce the dimension of a system by projecting the process variables to a lower-dimensional subspace of "scores" and removing the noise irrelevant to the process while still maintaining the important information about the process. Because a confidence level higher than 95% was achieved with two principal components, a two-dimensional score diagram as seen in Figure 6 could be used successfully to check the reliability of the results for new input data.

6. Conclusions

Industrial naphtha is the most important and frequently used feedstock of ethylene production in most non-oil-producing countries, but the composition of naphtha is not uniform or unique even for samples from the same mining site. Many petrochemical companies in non-oil-producing countries have purchased various naphtha feeds, but the economical efficiency could not be known because no mechanistic information relating the industrial indices and the conventional ethylene yield was available. There are two kinds of difficulties: one is the conversion from industrial indices to conventional molecules, and the other is the construction of a mechanism for the naphtha-pyrolysis reaction. For the former difficulty, an artificial neural network model was constructed on the basis of industrial naphtha analysis data, which shows good performance in characterizing naphtha. For the latter, the major reaction classes were identified, and for the identified important feed components, the major reaction paths were generated, and the kinetic parameters were compiled from all available open literature and kinetic theories. To diminish the computational load, the reaction mechanism was systematically reduced using the eigenvalue−eigenvector decomposition method, and further, it was tuned with real plant data. The constructed reaction mechanism is a mechanistic model, so that it can predict the product yields for various naphtha samples in a reliable manner. The reduced reaction mechanism with the feed characterization module can be used to determine the value of industrial naphtha from the industrial indices, such as PINAs, ASTM boiling curves, and specific gravities. It can also be very useful for the development of a full physical cracker model. The developed model can provide guidance in the purchasing of feedstock and in the of mixing various naphtha feeds and/or gas oils by predicting the product yield. Therefore, it can help to maximize the economic efficiency of naphtha cracking furnaces.

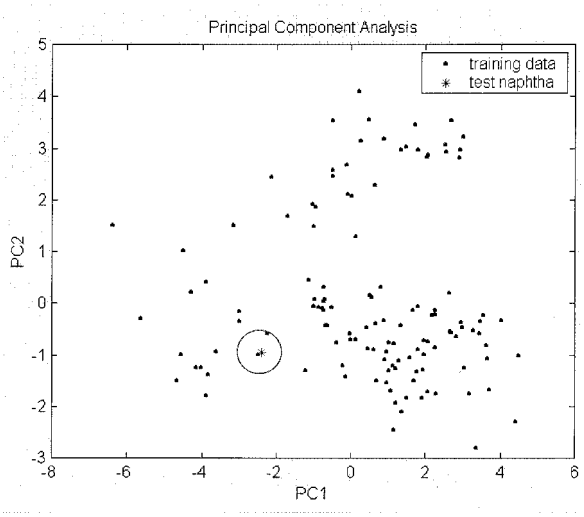

Figure 6. Score diagram for feed characterization.

Acknowledgment

The authors thank Dr. Jongku Lee of LG Chem. and Dr. Seungbin Park of KAIST for their helpful comments and discussions for this work. This work was also partially supported by the Brain Korea 21 project.

Nomenclature

s_{ij} = sensitivity of component i according to reaction j
c_i = concentration of component i

k_j = kinetic parameter of reaction j
y = state variables, concentrations and temperature
A = area (m^2)
T = temperature (K)
T_a = cracking coil surface temperature (K)
W = mass flow rate [kg/(m^2 s)]
V = linear velocity (m/s)
P = perimeter (m)
p = pressure (kPa)
f = friction factor
g = weight fraction of component (kg/kg)
f_{ij} = reaction amount of component i in reaction j [kg/(m^3 s)]
f_j = reaction amount of reaction j [kg/(m^3 s)]
U = overall heat-transfer coefficient [kJ/(m^2 s K)]
MW = molecular weight
NC = number of components
m = number of reactions
z = axial direction (m)
t = time (s)
ΔH = heat of reaction (kJ/kg)
C_p = heat capacity [kJ/(kg K)]
α = factor for overall heat-transfer coefficient
ρ = density (kg/m^3)
λ = eigenvalue
Ψ = principal component

Literature Cited

(1) Dente, M. D.; Ranzi, E. Mathematical modeling of hydrocarbon pyrolysis reactions. *Pyrolysis: Theory and Industrial Practice*; Albright, L. F., Crynes, B. L., Corcoran, W. H., Eds.; Academic Press: New York, 1983; Chapter 7.

(2) Kumar, P.; Kunzru, D. Modeling of naphtha pyrolysis. *Ind. Eng. Chem. Process Des. Dev.* **1985**, *24*, 774−782.

(3) Dente, M.; Ranzi, E.; Goossens, A. G. Detailed prediction of olefin yields from hydrocarbon pyrolysis through a fundamental simulation model (SPYRO). *Comput. Chem. Eng.* **1979**, *3*, 61−75.

(4) Van Damme, P. S.; Froment,G. F. Scaling up of naphtha cracking coils. *Ind. Eng. Chem. Process Des. Dev.* **1981**, *20*, 366−376.

(5) Kossiakoff, A.; Rice, R. O. Thermal decomposition of hydrocarbons, resonance stabilization and isomerization of free radicals. *J. Am. Chem. Soc.* **1943**, *65*, 590−595.

(6) Wagner, E. S.; Hamid, O. A.; Sohn, E. M.; Preston, R. F. PYROTEC's ethylene plant furnace modeling technology coupled with ASPENTECH's real-time optimization system provides off-line and on-line benefits. Presented at Aspen World, 1997.

(7) Ranzi, E.; Dente, M.; Pierucci, S.; Biardl, G. Initial product distributions from pyrolysis of normal and branched paraffins. *Ind. Eng. Chem. Fundam.* **1983**, *22*, 131−139.

(8) Ranzi, E.; Faravelli, T.; Gaffuri, P.; Garavaglian, E.; Goldaniga, A. Primary pyrolysis and oxidation reactions of linear and branched alkanes. *Ind. Eng. Chem. Res.* **1997**, *36*, 3336−3344.

(9) Murata, M.; Saito, S. A simulation model for high-conversion pyrolysis of normal paraffinic hydrocarbons. *J. Chem. Eng. Jpn.* **1975**, *8* (1), 39−45.

(10) Tomlin, A. S.; Pilling, M. J.; Merkin, J. H.; Brindley, J. Reduced mechanisms for propane pyrolysis. *Ind. Eng. Chem. Res.* **1995**, *34*, 3749−3760.

(11) Willems, P. A.; Froment, G. F. Kinetic modeling of the thermal cracking of hydrocarbons. 1. Calculation of frequency factors. *Ind. Eng. Chem. Res.* **1988**, *27*, 1959−1966.

(12) Nigam, A.; Klein, M. T. A mechanism-oriented lumping strategy for heavy hydrocarbon pyrolysis: imposition of quantitative structure−reactivity relationships for pure components. *Ind. Eng. Chem. Res.* **1993**, *32*, 1297−1303.

(13) Allara, D. L.; Shaw, R. A compilation of kinetic parameters for the thermal degradation of *n*-alkane molecules. *J. Phys. Chem. Ref. Data* **1980**, *9*, 523−559.

(14) Vajda, S.; Valko, P.; Turanyi, T. Principal component analysis of kinetic models. *Int. J. Chem.* **1985**, *17*, 55−81.

(15) Lutz, A. E.; Kee, R. J.; Miller, J. A. *SENKIN: A Fortran Program for Predicting Homogeneous Gas-Phase Chemical Kinetics with Sensitivity Analysis*; Report SAND87-8248; Sandia National Laboratories: Albuquerque, NM, 1988.

(16) Turanyi, T. Applications of sensitivity analysis to combustion chemistry. *Relat. Eng. Syst. Saf.* **1997**, *57*, 41−48.

(17) Gill, P. E.; Murray, W.; Saunders, M. A.; Wright, M. H. *User's Guide for NPSOL 5.0*; Technical Report SOL 86-1; Systems Optimization Laboratory: Stanford, CA, 1998.

(18) Brenan, K. E.; Campbell, S. L.; Petzold, L. R. *Numerical Solution of Initial Value Problems in Differential Algebraic Equations*; Elsevier: New York, 1989

(19) Kee, R. J.; Rupley, F. M.; Miller, J. A. *Chemkin-II: A Fortran Chemical Kinetics Package for the Analysis of Gas-Phase Chemical Kinetics*; Report SAND89-8009B, UC-706; Sandia National Laboratories: Livermore, CA, 1989

(20) *Technical Data Book—Petroleum Refining*, 4th ed.; American Petroleum Institute: Washington, D.C., 1983.

(21) Reide, R. C.; Prausnitz, J. M.; Poling, B. E. *The Properties of Gases and Liquids*, 4th ed.; McGraw-Hill: New York, 1987.

Received for review August 24, 2000
Revised manuscript received February 14, 2001
Accepted March 12, 2001

IE000774O